



The Preseason Warming of the Indian Ocean Resulting in Soybean Failure in U.S.

Menghan Li ^{1,3}, Xichen Li ^{1,2}, Yi Zhou ^{1,3}, and Yurong Hou ^{1,3}

5 ¹International Center for Climate and Environment Sciences, Institute of Atmospheric Physics, Chinese Academy of Sciences, Beijing, 100193, China.

²Institute of Ocean Research, Peking University, Beijing, 100193, China.

³University of Chinese Academy of Sciences, Beijing, 100193, China.

10 *Correspondence to:* Xichen Li (xichenli@pku.edu.cn)

Abstract. Soybean is the most important oilseed and feed crop globally. As one of the major soybean producers in the world, soybean yield variability in the United States has garnered widespread attention. We analyze the effect of the Indian Ocean sea surface temperature (SST) on soybean yield variability. Our findings indicate that variations in Indian Ocean SST during the November–December–January (hereinafter referred to as ND(-1)J) period, approximately nine months prior to harvest, account for 16% of the anomaly in U.S. soybean yields. Furthermore, for each standard deviation change in the Indian Ocean Basin (IOB) index, there is an estimated 4.0% change in total soybean production in the United States. The root zone soil moisture and maximum temperature during the reproductive growth stage in summer are the key factors influencing the United States soybean yields. The warming of the Indian Ocean could cause hot and dry conditions during July-August-September (JAS) by influencing ND(-1)J soil moisture and the eastern Pacific SST, leading to substantial soybean failures in the United States. Our findings emphasize the importance of the Indian Ocean SST on soybean production in the United States and reveal the pathways of this impact, which can help predict the United States soybean failures and improve food security worldwide.

1 Introduction

Soybeans are a vital oilseed and feed crop, providing essential proteins and fats for both human and animal nutrition worldwide. Due to their significant role, the distribution and trade of soybeans have attracted considerable attention, especially given the concentration of production in a few key countries. According to the Food and Agriculture Organization of the United Nations, in 2017, the United States, Brazil, and Argentina together produced approximately 75.8% of the global soybean supply, with the United States being the largest contributor. These three countries also dominate global soybean exports, accounting for over 80% of the total, with the U.S. alone representing more than 40% of exports between 2008 and 2012 (Birgit Meade et al., 2016; Torreggiani et al., 2018). This concentration underscores the importance of production fluctuations in these major soybean-producing nations.



Crop yields are influenced by various local meteorological factors, such as temperature, precipitation, solar radiation, soil moisture, and air humidity (Gaupp et al., 2020; Joshi et al., 2021; Li et al., 2019; Ray et al., 2015). However, for soybeans, hot and dry conditions during the critical reproductive phase in summer (July-August-September, JAS) are key factors leading to reduced yields (Hamed et al., 2021; Nendel et al., 2023; Teasdale & Cavigelli, 2017). For instance, Schauburger et al. (2017) have investigated the impact of high temperatures on the yields of US soybeans, which find that Each day with temperatures above 30°C reduces soybean yields by up to 6% under rainfed conditions and conclude that high temperatures negatively affect US crop yields primarily through water stress mechanisms. The risk of yield loss for soybeans due to drought is especially significant in the USA, with the likelihood of such losses potentially exceeding 70% during an exceptional drought (Leng & Hall, 2019). For example, the late summer of 2012 drought across the central U.S. caused soybean yields across the western Corn Belt and central Plains to be at least 25 percent below the long-term trend (Otkin et al., 2016).

Beyond immediate weather patterns, large-scale climate systems like the El Niño–Southern Oscillation (ENSO) also influence soybean yields by modulating seasonal temperature and precipitation patterns. Persistent La Niña phases, for example, can lead to soybean harvest failures across the U.S. and southeastern South America due to impacts on extratropical sea surface temperatures (SST) and spring soil moisture levels (Hamed et al., 2023). The effect of ENSO on soybean production has been widely studied (W. Anderson et al., 2017b; Nória Júnior et al., 2020; Perondi et al., 2022; Cao et al., 2023), revealing its significant role in soybean production.

Other climate oscillations, including the Atlantic Multidecadal Oscillation (AMO), Indian Ocean Basin (IOB), and North Atlantic Oscillation (NAO), also appear to influence weather conditions that affect soybean yields in the Americas (Gan et al., 2019; Manthos et al., 2022; F. Wang et al., 2013; C. Zhao & Brissette, 2022). For instance, a positive AMO phase is associated with warmer temperatures across North America, especially in the eastern regions (C. Zhao & Brissette, 2022). Meanwhile, warming of the tropical Indian Ocean basin corresponds with higher winter precipitation over southeastern South America, indicating the IOB’s significant influence on regional weather patterns (Hu et al., 2023). Despite these insights, the specific effects of these climate modes on soybean yields in the U.S. remain underexplored.

In this study, we investigate the correlation between multiple climate variability factors and U.S. soybean yields, identifying a significant influence from Indian Ocean SST anomalies. To quantify the direct and indirect impacts of IOB warming on U.S. soybean production, we first pinpoint the key climatic factors affecting yields. We then linked the Indian Ocean SST with these key factors and analyzed their teleconnection to elucidate its relationship with soybean yields in the United States. Our findings provide a valuable foundation for predicting soybean crop risks and for developing strategies to strengthen resilience in global soybean trade, thereby helping mitigate climate-related risks to food security.



60 2 Materials and Methods

2.1 Materials

The U.S. crop data used in this study includes harvest area, production, yield time series, and crop calendars, covering a 42-year period from 1978 to 2019. State-level soybean harvest data was obtained from the USDA's NASS Quick Stats database (<https://quickstats.nass.usda.gov/>), while planting and harvest dates at a 0.5-minute grid resolution were sourced from Sacks et al. (2010). Across the U.S., the primary soybean growing season typically spans May to November.

The annual U.S. soybean yield (Y_t) was calculated by aggregating yields across political units, weighted by harvested area. The formula is as follows:

$$Y_t = \frac{\sum Y_{t,s} \times Ha_{t,s}}{\sum Ha_{t,s}} \quad (1)$$

Where t and s denote the year and political unit, respectively, $Y_{t,s}$ and $Ha_{t,s}$ represent the yield (t/ha) and harvested area (ha).

70 To eliminate non-climatic influences on yield (W. Anderson et al., 2017a; Iizumi et al., 2014), we calculated expected yields ($Y_{Ext,s}$) by applying a five-year running mean for each state. The percent yield anomaly ($\Delta Y_{t,s}$) relative to expected yield was then computed as follows:

$$\Delta Y_{t,s} = \frac{Y_{t,s} - Y_{Ext,s}}{Y_{Ext,s}} \times 100 \quad (2)$$

Where t and s again represent the year and political unit, respectively. $Y_{t,s}$ represents the yield value (t/ha). Due to the five-year running mean (averaging from $t-2$ to $t+2$), anomalies could not be calculated for 1978, 1979, 2018, and 2019.

To capture the variability of the tropical Indian Ocean SST, we used monthly mean SST grid data at a $1.0^\circ \times 1.0^\circ$ resolution from the Hadley Centre Sea Ice and Sea Surface Temperature dataset (HadISST, Rayner et al., 2003) spanning 1979–2017. The IOB index was defined as the average SST anomaly (SSTA) in the region 20°S – 20°N , 40° – 110°E , while the Niño 3.4 index was calculated as the SSTA averaged over 5°S – 5°N , 170°W – 120°W . Prior to calculating these indices, SST fields were standardized by multiplying each value by the square root of the cosine of latitude.

To assess the impact of meteorological factors on soybean yields in the United States, we selected a set of indicators, including eight variables from the Climatic Research Unit (CRU) Time-series (TS) version 4.07 dataset (Harris et al., 2020): monthly mean gridded data ($0.25^\circ \times 0.25^\circ$) of maximum temperature (Tmx, $^\circ\text{C}$), mean temperature (Tmp, $^\circ\text{C}$), minimum temperature (Tmn, $^\circ\text{C}$), diurnal temperature range (DTR, $^\circ\text{C}$), mean precipitation (Pre, $\text{mm}\cdot\text{d}^{-1}$), surface downward short-wave radiation flux (DSRF, $\text{W}\cdot\text{m}^{-2}$), wet day frequency (wet, day), and cloud cover (Cld, %). Additionally, root zone soil moisture (SMroot, $\text{m}^3\cdot\text{m}^{-3}$) was sourced from the global climate of the European Centre for Medium-Range Weather Forecasts dataset (ERA5) (Hersbach et al., 2020). We also derived the vapor pressure deficit (VPD, hPa) as an additional indicator, calculated using the following formula:

$$e_0 = 6.108 \exp\left(\frac{17.27 \times \text{Tmp}}{\text{Tmp} + 237.3}\right) \quad (3)$$

$$\text{VPD} = e_0 - e_a \quad (4)$$



where T_{mp} is the monthly average temperature ($^{\circ}\text{C}$), and e_a is the average actual vapor pressure (hPa), both from the CRU dataset. e_0 represents the monthly mean saturated vapor pressure (hPa).

To investigate how the IOB mode influences key meteorological factors, we selected monthly values for mean sea level pressure (SLP, Pa), geopotential height at 200 hPa (GPH200, m), and wind components at 925 hPa (meridional, v_{925} in $\text{m}\cdot\text{s}^{-1}$, and zonal, u_{925} in $\text{m}\cdot\text{s}^{-1}$). SLP was obtained from the CRU dataset, while other variables were sourced from ERA5.

2.2 Statistical analyses

Before conducting a specific analysis, we used the Gram-Schmidt orthogonalization method to separate the effects of ENSO on climate indices and meteorological factors. By orthogonalizing ENSO with our variables, we can better isolate its influence, making the data easier to analyze.

We began by conducting a correlation analysis between multiple climate index time series and U.S. soybean yield data. In this step, we systematically adjusted the time range of each climate index to examine its lagging impact on soybean yield, which allowed us to identify the climate modes with the most significant influence. Next, we applied ridge regression to analyze the relationship between ten meteorological factors and soybean yield, isolating the three factors with the greatest impact on yield outcomes. We then divided the regression analysis into two components: (1) assessing the relationship between climate modes, key meteorological factors, and atmospheric circulation patterns, and (2) examining the link between key meteorological factors and soybean yield. This approach enabled us to construct an impact chain linking climate modes, weather conditions, and soybean yield.

3 Results

3.1 Climate variabilities and soybean yield anomalies

Many studies have focused on the climate variability of the Pacific and Atlantic Oceans, including phenomena such as ENSO and Tropical Atlantic variability (TAV), which will affect the weather conditions in the United States, resulting in fluctuations in soybean production (W. B. Anderson et al., 2019; Qian et al., 2020). However, in addition to these well-studied oceanic drivers, other climatic modes may also exert significant impacts on soybean yields. To explore this further, we conducted a comprehensive analysis of the correlation between soybean yields in key production regions and a broad range of climate indices. These indices include Niño3, Niño4, Niño3.4, Pacific North American Index (PNA), Pacific Decadal Oscillation (PDO), Southern Oscillation Index (SOI), AMO, Atlantic Meridional Mode (AMM), NAO, Tropical South Atlantic (TSA), Tropical North Atlantic (TNA), Indian Ocean Dipole (IOD), and IOB, among others. See Table S1 in the Supplementary for sources of these indices.

As shown in Fig. 1, during the soybean growth period (MAM-JAS), Niño3.4 and Niño4, which are associated with the ENSO phenomenon, exhibit a statistically significant correlation with U.S. soybean yields at the 95% confidence level based on a



two-tailed t-test. This finding aligns with previous studies, which have well-documented the influence of ENSO on soybean production (Anderson et al., 2017b; Hamed et al., 2023).

However, our analysis extends beyond the growing season to consider climate variability during the winter months prior to soybean planting. We find that the IOB mode, which captures large-scale warming or cooling in the Indian Ocean, plays a substantial role in determining soybean yields before sowing. The year-to-year anomalies in soybean yield exhibit a Pearson correlation coefficient of -0.41 with the IOB index during the ND(-1)J (November and December of the year preceding harvest and January of the harvest year), reaching statistical significance at the 99% confidence level based on a two-tailed t-test (Fig. 1). This suggests that the IOB mode accounts for approximately 16% of the interannual variability in soybean yield during this pre-growing season window.

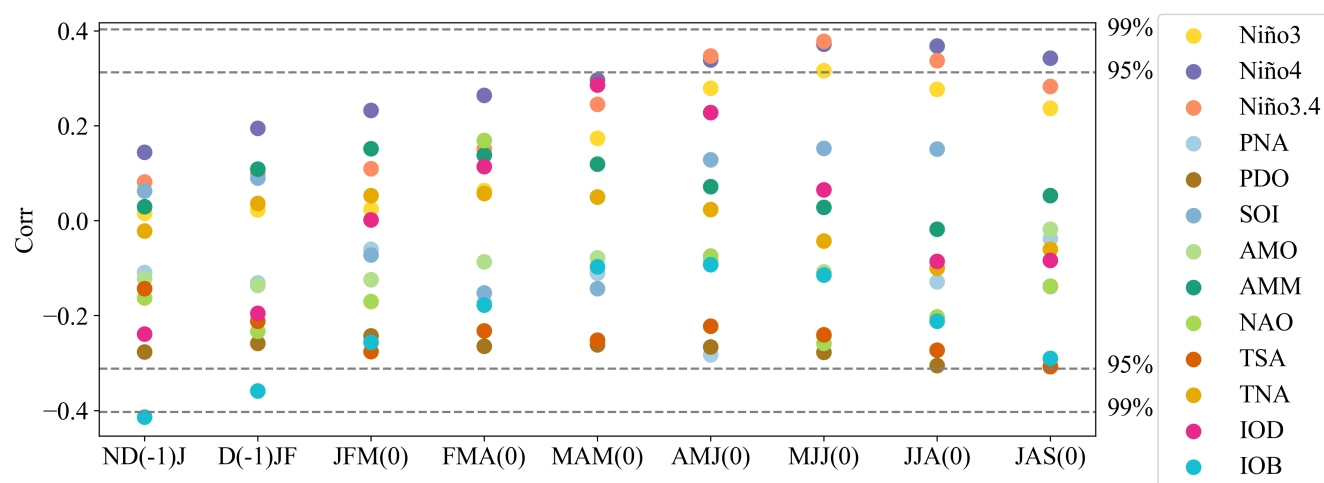


Figure 1: Correlation between the United States soybean yield anomalies and climate indices over 3-month periods from 1980 to 2017. The horizontal axis shows each 3-month window, and the vertical axis shows Pearson correlation coefficients. Colors represent different climate indices as listed in the legend. Dashed lines mark the vertical axis at the 95% and 99% significance levels based on the t-test.

Figure 2(a) illustrates the spatial distribution of soybean production in the United States. It is evident that soybean production is concentrated in the central United States, with Illinois, Iowa, Minnesota, Indiana, and Nebraska having the highest yields, accounting for more than 50% of the total soybean production in the country.

To explore how soybean yields respond to variations in the IOB mode across different U.S. regions, we conducted a regression analysis. The findings reveal that the IOB mode during ND(-1)J exerts a significant negative influence on soybean yields, with an inverse relationship between the IOB index and yields observed in most states (Fig. 2(b)). This negative correlation was especially pronounced in several key agricultural states. Notably, South Dakota, Kansas, Missouri, Illinois, Michigan, Indiana, Ohio, Kentucky, Tennessee, and New York displayed significant sensitivities to fluctuations in the IOB mode. The relationship between the IOB index and soybean yields in these regions passed the 90% significance threshold, indicating that the impact of the IOB mode on soybean production in these states is both statistically robust and consistent.



To quantify the overall impact of IOB fluctuations on U.S. soybean production, we calculated a weighted sum of the regression coefficients, with the weights based on the average harvested area and expected yields across individual regions. This approach provides a more comprehensive assessment of the IOB mode's effect on national production. The findings indicate that an increase in the IOB index is associated with a decrease in soybean production in nearly all regions of the United States (Fig. 2(c)). Specifically, a one standard deviation increase in the IOB index during ND(-1)J corresponds to a yield reduction of approximately 4.7 million tonnes in regions experiencing significant declines, while regions with notable yield increases were virtually nonexistent. Among these regions, Illinois saw the largest decline, with an estimated loss of around 800,000 tonnes. In aggregate, an increase of one standard deviation in the IOB index during ND(-1)J corresponds to a reduction of approximately 4.0% in total soybean production across the United States.

155

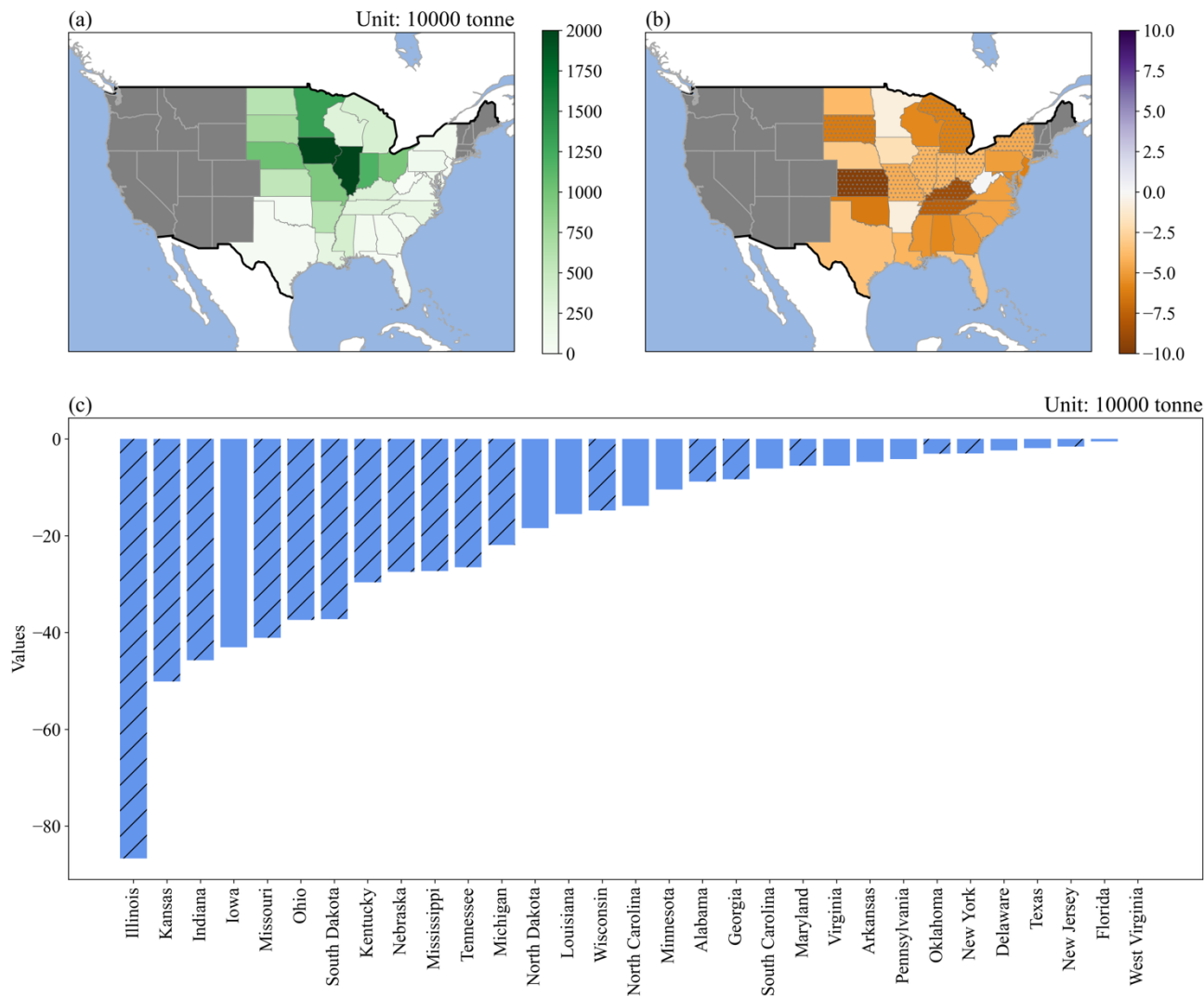


Figure 2: Spatial distribution of (a) average soybean production, (b) sensitivity of soybean yield anomalies (%), and (c) sensitivity of total soybean production (10,000 tonnes) to the IOB index during ND(-1)J from 1980 to 2017. Panel (a) shows the multi-year average production in each state. Panels (b) and (c) show the change in the percent yield anomaly and total production, respectively, per one standard deviation (1σ) increase in the standardized IOB index. The IOB index was standardized before analysis. Dots in (b) and striped bars in (c) indicate states where the correlation with the IOB index is statistically significant at the 90% confidence level based on the t-test.

3.2 Impacts of weather conditions on soybean yields

To identify the key factors influencing soybean yields in the United States, we focus on ten climate indicators: Tmp, Tmx, Tmn, DTR, DSRF, Pre, VPD, Cld, wet, and SMroot. It is crucial to recognize that these meteorological variables are



interrelated, meaning that each factor can influence and be influenced by others. For instance, elevated Tmx can increase evapotranspiration rates, reducing soil moisture. In turn, lower soil moisture limits evaporative cooling from the soil, which can elevate surface temperatures and decrease near-surface humidity (Miralles et al., 2014). Thus, the combined effects of these factors on soybean yields may be synergistic. To account for potential collinearity among meteorological variables, we applied ridge regression, which helps mitigate collinearity issues. The results revealed that DTR during the soybean reproductive stage (JAS) is the most critical determinant of soybean yield, followed by SMroot and Tmx (Table S2 in the Supplementary).

To more precisely assess the influence of these meteorological factors on soybean yields in the United States, we conducted a regression analysis examining their relationships with soybean yield across various states. Figure 3(a) demonstrates that an increase in the DTR is consistently associated with a decrease in soybean yields across nearly all regions of the United States. Statistically significant reductions in yields are observed in approximately 58% of the regions ($P < 0.1$), indicating that large temperature swings between day and night negatively affect soybean productivity. Figure 3(b) indicates a positive correlation between SMroot and soybean yields in most areas, particularly in the Midwest and Southeast, where significant positive correlations ($P < 0.1$) are evident. We also find that soybean yields are significantly impacted by DTR in areas similar to those affected by SMroot, suggesting that the effects of DTR are particularly pronounced in regions with limited water supply. Figure 3(c) illustrates that higher maximum temperatures (Tmx) are linked to decreased soybean yields in the southern and central United States, with significant negative correlations observed in these areas ($P < 0.1$). Notably, the spatial patterns of DTR and Tmx closely resemble each other, both showing an inverse relationship with SMroot.

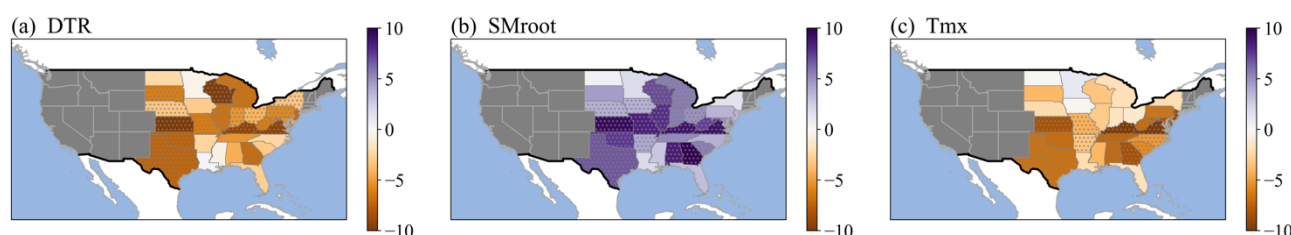


Figure 3: Sensitivity of soybean yield anomalies to (a) diurnal temperature range (DTR, °C), (b) root zone soil moisture (SMroot, $\text{m}^3 \cdot \text{m}^{-3}$), and (c) maximum temperature (Tmx, °C) during the growing season. Meteorological variables in this figure were standardized by removing the mean and dividing by the standard deviation before analysis. Values indicate the change in the percent yield anomaly (%) per one standard deviation (1σ) increase in each standardized variable. Dots denote correlations significant at the 90% confidence level (t-test).

3.3 Soil Moisture Memory Effect

During ND(-1)J, an increase in the IOB index results in a widespread reduction in SMroot across the United States. Significant soil moisture anomalies ($P < 0.1$) are particularly evident in North Dakota, South Dakota, Minnesota, Illinois, Georgia, South Carolina, North Carolina, and parts of Nebraska, Kansas, Iowa, Missouri, and Indiana (Fig. 4(e)). This decrease in SMroot



appears to be associated with anomalies in Pre and VPD, as regions experiencing reduced SMroot generally align with areas of increased VPD and decreased Pre.

As illustrated in Fig. 4(a), the warming signals from the Indian Ocean can affect the United States across the Pacific. The warming of the Indian Ocean enhances convective activities and upward motion, leading to the development of negative outgoing longwave radiation (OLR) anomalies. These anomalies generate Rossby waves that propagate from the tropical Indian Ocean to the United States via East Asia and the North Pacific (Hu et al., 2023; Ratnam et al., 2012). The response pattern of 200-hPa geopotential heights consists of a low–high system over the United States (Fig. 4(a)). This leads to southeasterly wind anomalies, which bring warmer and wetter equatorial air to the United States, causing widespread temperature increases in the United States and more precipitation in the southeastern United States (Fig. 4(b) and 4(c)). However, the southeasterly winds that bring warm and moist air shift to southwesterly winds in the northern United States (Fig. 4(a)), and the northeasterly wind anomaly transfers drier air from the polar regions to the Northern U.S. (F. Wang et al., 2013). Concurrently, the north-central United States becomes a water vapor divergence area (Fig. S2 in the Supplementary), reducing Pre and contributing to decreased SMroot in that area (Fig. 4(b) and 4(e)). In the southeastern United States, although Pre increases, the concurrent rise in Tmp intensifies VPD, contributing to the observed decrease in SMroot (Fig. 4(c)–(e)). Elevated Tmp could amplify VPD by accelerating soil and plant moisture loss, as shown in previous studies (Yin et al., 2014; F. Zhao et al., 2023).

For the root zone, soil moisture memory ranges from several days to up to a year and shows a long memory for dry soil moisture regimes (Stacke & Hagemann, 2016). A correlation analysis of soil moisture in ND(-1)J and JAS indicated that soil moisture during these periods was significantly correlated in regions with negative soil moisture anomalies in ND(-1)J (Fig. S3 in the Supplementary). Therefore, the decrease in SMroot during the ND(-1)J period can affect SMroot levels during the soybean reproductive growth phase via the soil memory effect, thereby influencing soybean yield.

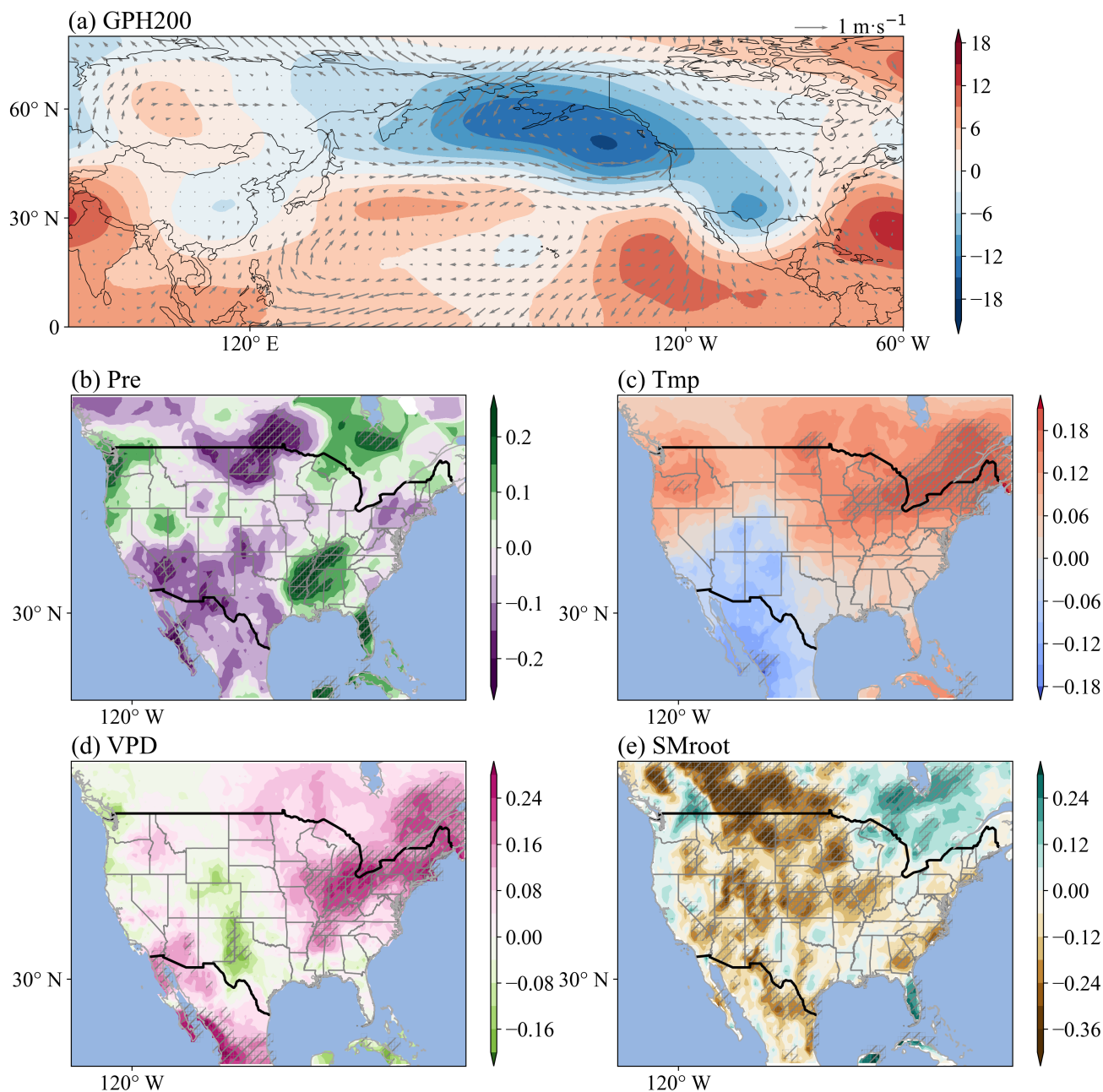


Figure 4: Responses of (a) 200 hPa geopotential height (GPH200, m), (b) precipitation (Pre, $\text{mm}\cdot\text{d}^{-1}$), (c) mean temperature (Tmp, $^{\circ}\text{C}$), (d) vapor pressure deficit (VPD, hPa), and (e) root zone soil moisture (SMroot, $\text{m}^3\cdot\text{m}^{-3}$) to the IOB index during ND(-1)J. Vectors in (a) show wind responses at 925 hPa ($\text{m}\cdot\text{s}^{-1}$) to a 1σ increase in the standardized IOB index. All variables except GPH200 and winds were standardized before analysis. Color bar values in (a) represent changes in GPH200 (m) per 1σ increase in the standardized IOB index, while color bar values in (b–e) represent standardized changes (in σ units) in meteorological variables per 1σ increase in the standardized IOB index. Shaded areas with diagonal hatching indicate regions where the response is statistically significant at the 90% confidence level (t-test).



225

3.4 Sea Surface Temperature Feedback Effect

The warming of the Indian Ocean during the ND(-1)J could indirectly influence JAS meteorological conditions in the United States by affecting Pacific SSTs. It is associated with a Matsuno-Gill-type response, which excites atmospheric Kelvin waves propagating eastward (Gill, 1980; Matsuno, 1966). This results in easterly wind anomalies over the western-central equatorial Pacific. Strengthened easterly winds lead to a shallower thermocline, which brings colder waters closer to the surface, contributing to the cooling of SSTs in the eastern Pacific. This cooling effect can persist throughout the summer months, as illustrated in Fig. 5(a), and is a key component of the development of La Niña events (Cai et al., 2019; C. Wang, 2019; Wu & Kirtman, 2004; Xie et al., 2016). During La Niña events, there are significant atmospheric circulation anomalies that further impact the United States. For example, Fig. 5(b) shows that during La Niña years, 200 hPa geopotential height anomalies are predominantly positive in the mid-latitudes, while negative anomalies occur in the tropics and certain high-latitude regions (Luo & Lau, 2020). These geopotential height anomalies reflect the establishment of an anomalous high-pressure system over much of the United States.

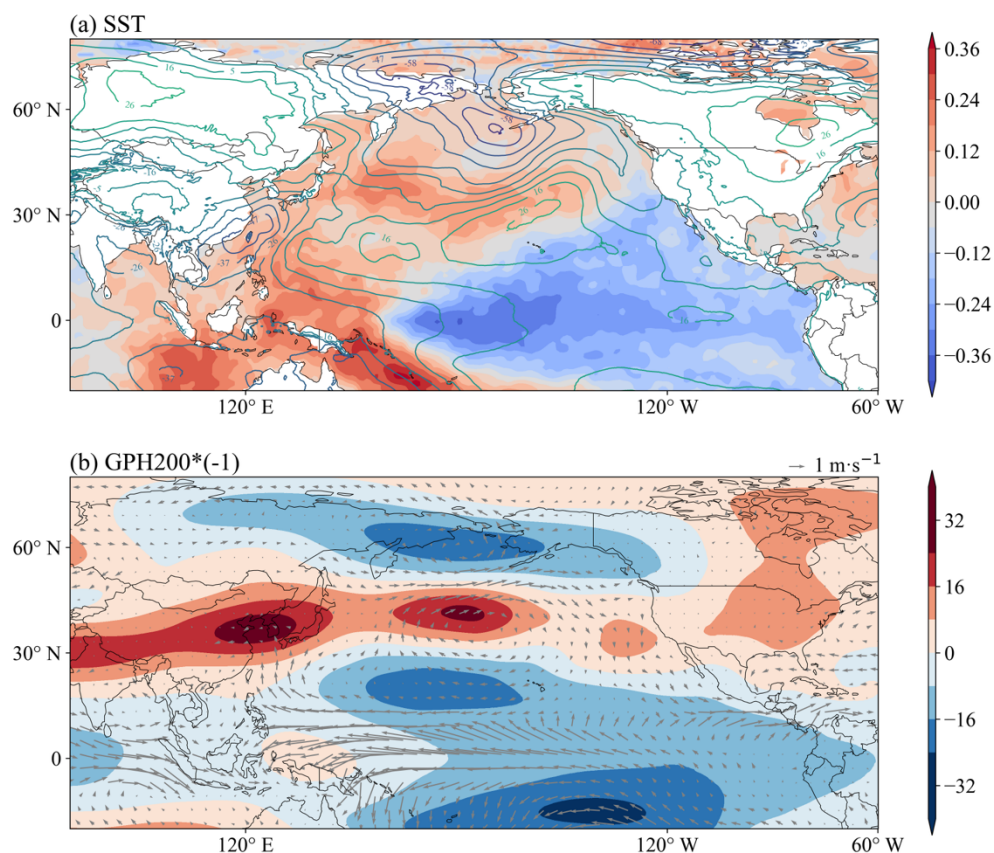
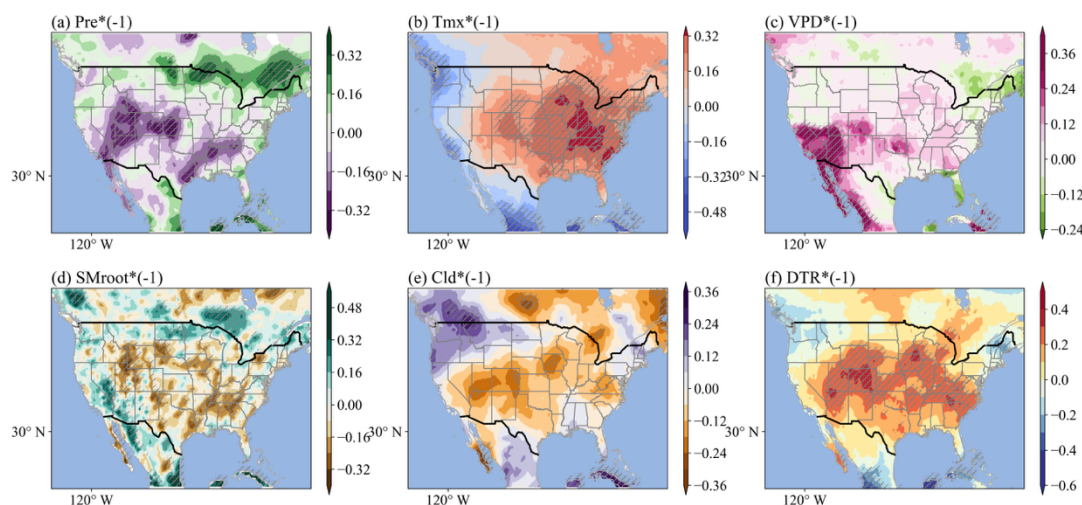




Figure 5: (a) Correlation between sea surface temperature (SST, °C) and the IOB index, and (b) responses of 200 hPa geopotential height anomalies (GPH200, m) to the Niño3.4 index during JAS. Solid contours in (a) represent sea level pressure (SLP) anomalies (units: Pa). Vectors in (a) show wind responses at 925 hPa ($\text{m}\cdot\text{s}^{-1}$) to a 1σ decrease in the standardized IOB index. GPH200, winds, and SLP are shown in original units; the IOB and Niño3.4 indices were standardized before analysis. Color bar values in (a) represent correlation coefficients; color bar values in (b) represent the change in GPH200 (m) per 1σ decrease in the standardized Niño3.4 index.

Such conditions lead to changes in meteorological patterns across the United States, including warmer temperature anomalies and decreased precipitation (Jia et al., 2016; Jong et al., 2020, 2021; Mo et al., 2009; Z. Wang et al., 2007). Consequently, substantial reductions in Pre and increases in Tmx are shown in Fig. 6(a) and 6(b). The elevated Tmx exacerbates evapotranspiration, driving higher moisture loss from both the soil and the plants. This warming effect intensifies the drought-like conditions across several regions of the United States. Additionally, a noticeable rise in the VPD (Fig. 6(c)) further compounds the stress on crops by increasing the demand for moisture in the atmosphere. This heightened atmospheric moisture deficit, combined with reduced precipitation, directly leads to declining SMroot levels (Fig. 6(d)). These patterns indicate a clear decline in soil water availability, heightening the risk of drought conditions across affected regions. Moreover, Fig. 6(e) reveals a significant increase in the DTR across soybean-growing regions. This increase is likely associated with a reduction in Cld (Fig. 6(g)), which allows for more extreme temperature variations between day and night. The pattern observed in this study is similar to those examined by Doan et al. (2022).

These results indicate that the variability of the IOB can affect the meteorological elements in the United States by influencing the development of ENSO. The hot and dry conditions resulting from these meteorological changes are particularly detrimental to soybean yields, as highlighted by Anderson et al. (2017a) and Hamed et al. (2023). The combined impacts of increased Tmx and DTR, decreased Pre, elevated VPD, and reduced SMroot create an environment highly unfavorable for soybean production. This highlights the critical role of these climate drivers in influencing agricultural outcomes under positive IOB conditions (Fig. S4 in the Supplementary).





265 **Figure 6: Responses of (a) precipitation (Pre, mm·d⁻¹), (b) maximum temperature (Tmx, °C), (c) vapor pressure deficit (VPD, hPa), (d) root zone soil moisture (SMroot, m³·m⁻³), (e) cloud cover (Cld, %), and (f) diurnal temperature range (DTR, °C) to the Niño3.4 index during JAS. All variables were standardized before analysis. Values indicate the standardized change (in σ units) in meteorological variables per 1 σ decrease in the standardized Niño3.4 index. Shaded areas with diagonal hatching indicate regions where the response is statistically significant at the 90% confidence level (t-test).**

270 4 Summary and discussion

This study examines the significant impact of Indian Ocean basin-wide SST anomalies on the United States soybean yields. The IOB mode during the winter before the growing season (ND(-1)J) explains about 16% of soybean yield variability. The warming of the Indian Ocean is linked to atmospheric Rossby waves that affect temperature and precipitation patterns in the United States, influencing soil moisture and contributing to hot and dry conditions during the reproductive season. The findings suggest that the IOB index could be a useful predictor for soybean yields, aiding in proactive decision-making for food security and trade policies.

Previous studies have predicted crop yield based on early signals of ENSO and explained the lagged impact of that on crop yield through soil moisture memory and sea surface temperature memory (W. Anderson et al., 2017b; Cao et al., 2023; Hamed et al., 2023; Von Bloh et al., 2023). While ENSO is a major driver of global climate, its interactions with other climate systems (Cai et al., 2019; Fan & Meng, 2023; Strong et al., 2020; Zhang et al., 2022), like the Indian Ocean, have been overlooked. This study is the first to highlight the significant impact of the IOB index on the United States soybean yields, identifying the IOB as a key predictive factor with a nine-month lead time, exceeding the influence of ENSO. Our findings offer early warnings of potential yield reductions, enabling farmers to adapt management practices and guiding governments in adjusting trade policies to mitigate climate-related risks.

285 This study has uncertainties due to the restricted availability of agricultural and meteorological data, analyzing only 38 years, which may introduce potential errors. Varying spatial scales of crop statistics and scarce data in some regions could also affect accuracy. Additionally, while precipitation and temperature are commonly used (Lobell et al., 2011; Mourtzinis et al., 2015; Ray et al., 2015), more specific agroclimatic indices may provide better insights into climate-crop relationships. The complexity of crop yield variability, influenced by multiple interacting climate modes, requires a combined analysis of key factors. Non-climatic factors, such as agricultural practices and crop genetics, should also be integrated into future yield predictions for greater accuracy.

Our study is the first to highlight the impact of the Indian Ocean on agriculture in the United States, advancing our understanding of ocean-atmosphere-agriculture interactions. Our findings offer a new and feasible approach to predicting soybean production in the United States, providing essential guidance for soybean-exporting countries to enhance their export competitiveness and for importing countries to diversify their supply chains. The ability to predict soybean yields with a lead time of nine months can significantly aid in strategic planning and decision-making, potentially reducing the economic impact



of adverse climate conditions on the agricultural sector. Furthermore, this research underscores the importance of continuous monitoring and modeling of global climate systems to better anticipate and respond to the challenges posed by climate change.

Data availability

300 The U.S. State-level soybean harvest data was obtained from the USDA's NASS Quick Stats database (<https://quickstats.nass.usda.gov/>). The crop planting and harvest dates were obtained from Crop Calendar Dataset (Sacks et al., 2010). Monthly mean SST grid data from the Hadley Centre Sea Ice and Sea Surface Temperature dataset (Rayner et al., 2003). Monthly gridded maximum temperature, mean temperature, minimum temperature, diurnal temperature range, mean precipitation, surface downward short-wave radiation flux, wet day frequency, vapor pressure, cloud cover, and mean sea
305 level pressure were obtained from the Climatic Research Unit (CRU) v4.07 dataset (Harris et al., 2020). The monthly root zone soil moisture, geopotential height at 200 hPa, and wind components at 925 hPa is publicly available from the European Centre for Medium-Range Weather Forecasts dataset (ERA5, Hersbach et al., 2020).

Author contribution

Menghan Li was involved in data curation; formal analysis; investigation; methodology; visualization; writing-original draft;
310 and writing-review and editing. Yi Zhou was involved in writing-review and editing. Yurong Hou was involved in Validation. Xichen Li was involved in conceptualization; supervision; and writing-review and editing.

Competing interests

The authors declare no conflict of interest relevant to this study.

315 References

- Anderson, W., Seager, R., Baethgen, W., and Cane, M.: Crop production variability in North and South America forced by life-cycles of the El Niño Southern Oscillation, *Agricultural and Forest Meteorology*, 239, 151–165, <https://doi.org/10.1016/j.agrformet.2017.03.008>, 2017a.
- Anderson, W., Seager, R., Baethgen, W., and Cane, M.: Life cycles of agriculturally relevant ENSO teleconnections in North
320 and South America, *Intl Journal of Climatology*, 37, 3297–3318, <https://doi.org/10.1002/joc.4916>, 2017b.
- Anderson, W., Seager, R., Baethgen, W., Cane, M., and You, L.: Synchronous crop failures and climate-forced production variability, *Sci. Adv.*, 5, eaaw1976, <https://doi.org/10.1126/sciadv.aaw1976>, 2019.



- Birgit Meade, Estefanía Puricelli, William McBride, Constanza Valdes, Linwood Hoffman, Linda Foreman, and Erik Dohlman: Corn and Soybean Production Costs and Export Competitiveness in Argentina, Brazil, and the United States, Social Science Research Network, Rochester, NY, USA, 2016.
- Cai, W., Wu, L., Lengaigne, M., Li, T., McGregor, S., Kug, J.-S., Yu, J.-Y., Stuecker, M. F., Santoso, A., Li, X., Ham, Y.-G., Chikamoto, Y., Ng, B., McPhaden, M. J., Du, Y., Dommenges, D., Jia, F., Kajtar, J. B., Keenlyside, N., Lin, X., Luo, J.-J., Martín-Rey, M., Ruprich-Robert, Y., Wang, G., Xie, S.-P., Yang, Y., Kang, S. M., Choi, J.-Y., Gan, B., Kim, G.-I., Kim, C.-E., Kim, S., Kim, J.-H., and Chang, P.: Pantropical climate interactions, *Science*, 363, eaav4236, <https://doi.org/10.1126/science.aav4236>, 2019.
- Cao, J., Zhang, Z., Tao, F., Chen, Y., Luo, X., and Xie, J.: Forecasting global crop yields based on El Niño Southern Oscillation early signals, *Agricultural Systems*, 205, 103564, <https://doi.org/10.1016/j.agsy.2022.103564>, 2023.
- Doan, Q., Chen, F., Asano, Y., Gu, Y., Nishi, A., Kusaka, H., and Niyogi, D.: Causes for Asymmetric Warming of Sub-Diurnal Temperature Responding to Global Warming, *Geophysical Research Letters*, 49, e2022GL100029, <https://doi.org/10.1029/2022GL100029>, 2022.
- Fan, L. and Meng, X.: The Asymmetric Predictive Power of Indian Ocean Dipole for Subsequent Year's ENSO: Role of Atlantic Ocean as an Intermediary, *Geophysical Research Letters*, 50, e2023GL105525, <https://doi.org/10.1029/2023GL105525>, 2023.
- Gan, Z., Guan, X., Kong, X., Guo, R., Huang, H., Huang, W., and Xu, Y.: The Key Role of Atlantic Multidecadal Oscillation in Minimum Temperature Over North America During Global Warming Slowdown, *Earth and Space Science*, 6, 387–397, <https://doi.org/10.1029/2018EA000443>, 2019.
- Gaupp, F., Hall, J., Hochrainer-Stigler, S., and Dadson, S.: Changing risks of simultaneous global breadbasket failure, *Nat. Clim. Chang.*, 10, 54–57, <https://doi.org/10.1038/s41558-019-0600-z>, 2020.
- Gill, A. E.: Some simple solutions for heat-induced tropical circulation, *Quart J Royal Meteorol Soc*, 106, 447–462, <https://doi.org/10.1002/qj.49710644905>, 1980.
- Hamed, R., Van Loon, A. F., Aerts, J., and Coumou, D.: Impacts of compound hot–dry extremes on US soybean yields, *Earth Syst. Dynam.*, 12, 1371–1391, <https://doi.org/10.5194/esd-12-1371-2021>, 2021.
- Hamed, R., Vijverberg, S., Van Loon, A. F., Aerts, J., and Coumou, D.: Persistent La Niñas drive joint soybean harvest failures in North and South America, *Earth Syst. Dynam.*, 14, 255–272, <https://doi.org/10.5194/esd-14-255-2023>, 2023.
- Harris, I., Osborn, T. J., Jones, P., and Lister, D.: Version 4 of the CRU TS monthly high-resolution gridded multivariate climate dataset, *Sci Data*, 7, 109, <https://doi.org/10.1038/s41597-020-0453-3>, 2020.
- Hersbach, H., Bell, B., Berrisford, P., Hirahara, S., Horányi, A., Muñoz-Sabater, J., Nicolas, J., Peubey, C., Radu, R., Schepers, D., Simmons, A., Soci, C., Abdalla, S., Abellan, X., Balsamo, G., Bechtold, P., Biavati, G., Bidlot, J., Bonavita, M., De Chiara, G., Dahlgren, P., Dee, D., Diamantakis, M., Dragani, R., Flemming, J., Forbes, R., Fuentes, M., Geer, A., Haimberger, L., Healy, S., Hogan, R. J., Hólm, E., Janisková, M., Keeley, S., Laloyaux, P., Lopez, P., Lupu, C., Radnoti, G., De Rosnay, P.,



- Rozum, I., Vamborg, F., Villaume, S., and Thépaut, J.: The ERA5 global reanalysis, *Quart J Royal Meteor Soc*, 146, 1999–2049, <https://doi.org/10.1002/qj.3803>, 2020.
- Hu, Z.-Z., Kumar, A., Jha, B., Chen, M., and Wang, W.: The tropical Indian Ocean matters for U. S. winter precipitation variability and predictability, *Environ. Res. Lett.*, 18, 074033, <https://doi.org/10.1088/1748-9326/ace06e>, 2023.
- 360 Iizumi, T., Luo, J.-J., Challinor, A. J., Sakurai, G., Yokozawa, M., Sakuma, H., Brown, M. E., and Yamagata, T.: Impacts of El Niño Southern Oscillation on the global yields of major crops, *Nat Commun*, 5, 3712, <https://doi.org/10.1038/ncomms4712>, 2014.
- Jia, L., Vecchi, G. A., Yang, X., Gudgel, R. G., Delworth, T. L., Stern, W. F., Paffendorf, K., Underwood, S. D., and Zeng, F.: The Roles of Radiative Forcing, Sea Surface Temperatures, and Atmospheric and Land Initial Conditions in U.S. Summer Warming Episodes, *Journal of Climate*, 29, 4121–4135, <https://doi.org/10.1175/JCLI-D-15-0471.1>, 2016.
- 365 Jong, B.-T., Ting, M., Seager, R., and Anderson, W. B.: ENSO Teleconnections and Impacts on U.S. Summertime Temperature during a Multiyear La Niña Life Cycle, *Journal of Climate*, 33, 6009–6024, <https://doi.org/10.1175/JCLI-D-19-0701.1>, 2020.
- Jong, B.-T., Ting, M., and Seager, R.: Assessing ENSO Summer Teleconnections, Impacts, and Predictability in North America, *Journal of Climate*, 34, 3629–3643, <https://doi.org/10.1175/JCLI-D-20-0761.1>, 2021.
- 370 Joshi, V. R., Kazula, M. J., Coulter, J. A., Naeve, S. L., and Garcia Y Garcia, A.: In-season weather data provide reliable yield estimates of maize and soybean in the US central Corn Belt, *Int J Biometeorol*, 65, 489–502, <https://doi.org/10.1007/s00484-020-02039-z>, 2021.
- Leng, G. and Hall, J.: Crop yield sensitivity of global major agricultural countries to droughts and the projected changes in the future, *Science of The Total Environment*, 654, 811–821, <https://doi.org/10.1016/j.scitotenv.2018.10.434>, 2019.
- 375 Li, Y., Guan, K., Schnitkey, G. D., DeLucia, E., and Peng, B.: Excessive rainfall leads to maize yield loss of a comparable magnitude to extreme drought in the United States, *Global Change Biology*, 25, 2325–2337, <https://doi.org/10.1111/gcb.14628>, 2019.
- Lobell, D. B., Schlenker, W., and Costa-Roberts, J.: Climate Trends and Global Crop Production Since 1980, *Science*, 333, 616–620, <https://doi.org/10.1126/science.1204531>, 2011.
- 380 Luo, M. and Lau, N.-C.: Summer heat extremes in northern continents linked to developing ENSO events, *Environ. Res. Lett.*, 15, 074042, <https://doi.org/10.1088/1748-9326/ab7d07>, 2020.
- Manthos, Z. H., Pegion, K. V., Dirmeyer, P. A., and Stan, C.: The relationship between surface weather over North America and the Mid-Latitude Seasonal Oscillation, *Dynamics of Atmospheres and Oceans*, 99, 101314, <https://doi.org/10.1016/j.dynatmoce.2022.101314>, 2022.
- 385 Matsuno, T.: Quasi-Geostrophic Motions in the Equatorial Area, *Journal of the Meteorological Society of Japan*, 44, 25–43, https://doi.org/10.2151/jmsj1965.44.1_25, 1966.
- Miralles, D. G., Teuling, A. J., Van Heerwaarden, C. C., and Vilà-Guerau De Arellano, J.: Mega-heatwave temperatures due to combined soil desiccation and atmospheric heat accumulation, *Nature Geosci*, 7, 345–349, <https://doi.org/10.1038/ngeo2141>, 2014.



- 390 Mo, K. C., Schemm, J.-K. E., and Yoo, S.-H.: Influence of ENSO and the Atlantic Multidecadal Oscillation on Drought over the United States, *Journal of Climate*, 22, 5962–5982, <https://doi.org/10.1175/2009JCLI2966.1>, 2009.
- Mourtzinis, S., Specht, J. E., Lindsey, L. E., Wiebold, W. J., Ross, J., Nafziger, E. D., Kandel, H. J., Mueller, N., Devillez, P. L., Arriaga, F. J., and Conley, S. P.: Climate-induced reduction in US-wide soybean yields underpinned by region- and in-season-specific responses, *Nature Plants*, 1, 14026, <https://doi.org/10.1038/nplants.2014.26>, 2015.
- 395 Nendel, C., Reckling, M., Debaeke, P., Schulz, S., Berg-Mohnicke, M., Constantin, J., Fronzek, S., Hoffmann, M., Jakšić, S., Kersebaum, K., Klimek-Kopyra, A., Raynal, H., Schoving, C., Stella, T., and Battisti, R.: Future area expansion outweighs increasing drought risk for soybean in Europe, *Global Change Biology*, 29, 1340–1358, <https://doi.org/10.1111/gcb.16562>, 2023.
- Nóia Júnior, R. D. S., Fraisse, C. W., Karrei, M. A. Z., Cerbaro, V. A., and Perondi, D.: Effects of the El Niño Southern Oscillation phenomenon and sowing dates on soybean yield and on the occurrence of extreme weather events in southern Brazil, *Agricultural and Forest Meteorology*, 290, 108038, <https://doi.org/10.1016/j.agrformet.2020.108038>, 2020.
- Otkin, J. A., Anderson, M. C., Hain, C., Svoboda, M., Johnson, D., Mueller, R., Tadesse, T., Wardlow, B., and Brown, J.: Assessing the evolution of soil moisture and vegetation conditions during the 2012 United States flash drought, *Agricultural and Forest Meteorology*, 218–219, 230–242, <https://doi.org/10.1016/j.agrformet.2015.12.065>, 2016.
- 405 Perondi, D., De Souza Nóia Júnior, R., Zotarelli, L., Mulvaney, M. J., and Fraisse, C. W.: Soybean maturity groups and sowing dates to minimize ENSO and extreme weather events effects on yield variability in the Southeastern US, *Agricultural and Forest Meteorology*, 324, 109104, <https://doi.org/10.1016/j.agrformet.2022.109104>, 2022.
- Qian, Y., Zhao, J., Zheng, S., Cao, Y., and Xue, L.: Risk assessment of the global crop loss in ENSO events, *Physics and Chemistry of the Earth, Parts A/B/C*, 116, 102845, <https://doi.org/10.1016/j.pce.2020.102845>, 2020.
- 410 Ratnam, J. V., Behera, S. K., Masumoto, Y., and Yamagata, T.: Role of Rossby Waves in the Remote Effects of the North Indian Ocean Tropical Disturbances, *Monthly Weather Review*, 140, 3620–3633, <https://doi.org/10.1175/MWR-D-12-00027.1>, 2012.
- Ray, D. K., Gerber, J. S., MacDonald, G. K., and West, P. C.: Climate variation explains a third of global crop yield variability, *Nat Commun*, 6, 5989, <https://doi.org/10.1038/ncomms6989>, 2015.
- 415 Rayner, N. A., Parker, D. E., Horton, E. B., Folland, C. K., Alexander, L. V., Rowell, D. P., Kent, E. C., and Kaplan, A.: Global analyses of sea surface temperature, sea ice, and night marine air temperature since the late nineteenth century, *J. Geophys. Res.*, 108, 2002JD002670, <https://doi.org/10.1029/2002JD002670>, 2003.
- Sacks, W. J., Deryng, D., Foley, J. A., and Ramankutty, N.: Crop planting dates: an analysis of global patterns, *Global Ecology and Biogeography*, 19, 607–620, <https://doi.org/10.1111/j.1466-8238.2010.00551.x>, 2010.
- 420 Stacke, T. and Hagemann, S.: Lifetime of soil moisture perturbations in a coupled land–atmosphere simulation, *Earth Syst. Dynam.*, 7, 1–19, <https://doi.org/10.5194/esd-7-1-2016>, 2016.
- Strong, C., McCabe, G. J., and Weech, A.: Step Increase in Eastern U.S. Precipitation Linked to Indian Ocean Warming, *Geophysical Research Letters*, 47, e2020GL088911, <https://doi.org/10.1029/2020GL088911>, 2020.



- Teasdale, J. R. and Cavigelli, M. A.: Meteorological fluctuations define long-term crop yield patterns in conventional and
425 organic production systems, *Sci Rep*, 7, 688, <https://doi.org/10.1038/s41598-017-00775-8>, 2017.
- Torreggiani, S., Mangioni, G., Puma, M. J., and Fagiolo, G.: Identifying the community structure of the food-trade international
multi-network, *Environ. Res. Lett.*, 13, 054026, <https://doi.org/10.1088/1748-9326/aabf23>, 2018.
- Von Bloh, M., Nória Júnior, R. D. S., Wangerpohl, X., Saltik, A. O., Haller, V., Kaiser, L., and Asseng, S.: Machine learning
for soybean yield forecasting in Brazil, *Agricultural and Forest Meteorology*, 341, 109670,
430 <https://doi.org/10.1016/j.agrformet.2023.109670>, 2023.
- Wang, C.: Three-ocean interactions and climate variability: a review and perspective, *Clim Dyn*, 53, 5119–5136,
<https://doi.org/10.1007/s00382-019-04930-x>, 2019.
- Wang, F., Liu, Z., and Notaro, M.: Extracting the Dominant SST Modes Impacting North America’s Observed Climate*,
Journal of Climate, 26, 5434–5452, <https://doi.org/10.1175/JCLI-D-12-00583.1>, 2013.
- 435 Wang, Z., Chang, C.-P., and Wang, B.: Impacts of El Niño and La Niña on the U.S. Climate during Northern Summer, *Journal*
of Climate, 20, 2165–2177, <https://doi.org/10.1175/JCLI4118.1>, 2007.
- Wu, R. and Kirtman, B. P.: Understanding the Impacts of the Indian Ocean on ENSO Variability in a Coupled GCM, *J. Climate*,
17, 4019–4031, [https://doi.org/10.1175/1520-0442\(2004\)017<4019:UTIOTI>2.0.CO;2](https://doi.org/10.1175/1520-0442(2004)017<4019:UTIOTI>2.0.CO;2), 2004.
- Xie, S.-P., Kosaka, Y., Du, Y., Hu, K., Chowdary, J. S., and Huang, G.: Indo-western Pacific ocean capacitor and coherent
440 climate anomalies in post-ENSO summer: A review, *Adv. Atmos. Sci.*, 33, 411–432, <https://doi.org/10.1007/s00376-015-5192-6>, 2016.
- Yin, D., Roderick, M. L., Leech, G., Sun, F., and Huang, Y.: The contribution of reduction in evaporative cooling to higher
surface air temperatures during drought, *Geophysical Research Letters*, 41, 7891–7897,
<https://doi.org/10.1002/2014GL062039>, 2014.
- 445 Zhang, Y., Li, J., Hou, Z., Zuo, B., Xu, Y., Tang, X., and Wang, H.: Climatic Effects of the Indian Ocean Tripole on the
Western United States in Boreal Summer, *Journal of Climate*, 35, 2503–2523, <https://doi.org/10.1175/JCLI-D-21-0490.1>, 2022.
- Zhao, C. and Brissette, F.: Impacts of large-scale oscillations on climate variability over North America, *Climatic Change*,
173, 4, <https://doi.org/10.1007/s10584-022-03383-2>, 2022.
- Zhao, F., Wang, G., Li, S., Hagan, D. F. T., and Ullah, W.: The combined effects of VPD and soil moisture on historical maize
450 yield and prediction in China, *Front. Environ. Sci.*, 11, 1117184, <https://doi.org/10.3389/fenvs.2023.1117184>, 2023.